# Synthesis of Inorganic and Metallic Nanoparticles by Miniemulsification of Molten Salts and Metals

Mirjam Willert, Regina Rothe, Katharina Landfester,* and Markus Antonietti

*Max-Planck-Institute of Colloids and Interfaces, Research Campus Golm, 14424 Potsdam, Germany*

*Received May 17, 2001*

A new and extraordinarily convenient route for the synthesis of nanoparticulate salts, metals, and metal oxides is presented. This technique is based on a liquid−liquid technology, namely, the miniemulsification of a molten or precursor state and subsequent heterophase reaction toward the desired product. First, data on the synthesis of iron oxide, magnetite, zirconia, and calcium carbonate are presented. The miniemulsification process is also suited to prepare metallic nanoparticles by using gallium or alloys with a low melting point.

## Introduction

Finely dispersed metal salts and nanoparticles are widely used in numerous technological and medical applications, e.g., as ceramic precursors, filler materials, pigments, recording materials, electronics, catalysts, medical diagnostics, and many others. Several techniques have been developed for the generation of such particles, some based on physical and some on chemical principles. With mechanical grinding or so-called colloidal milling, particles smaller than 1 $\mu$m are not accessible; the grain distribution is broad, and the shape is irregular due to the nondirected cracking. This is why wet chemical procedures are of larger importance, since they allow, in principle, control of size and shape.

One of the water-born techniques which leads to monodisperse inorganic particles with variable shape is the controlled precipitation from homogeneous electrolyte solutions.[1] For the preparation of crystalline α-alumina and boehmite particles, Sharma et al. combined coprecipitation and hydrothermal treatment.[2] In most cases, precipitation, however, is obtained in rather dilute solutions and is restricted to materials which can be precipitated, which means that the solubility can be changed by the addition of a second reactant.

Another class of wet chemical processes regularly found in the literature employ inverse microemulsions or inverse micelles.[3,4] Here, both nanoparticles and nanostructures are synthesized in the polar pools of ordered mesophases in an organic medium. Usually, two separate microemulsions, each consisting of one of the precursors to be reacted, are mixed together, and the reaction leading to the solid is induced by micellar-exchange processes.[3] The size of the nanoparticles can be varied by the amount of surfactant and solubilized water in the reverse micellar phase.[5] It is noted that both reductions as well as precipitations can be performed and that the generated nanoparticles are usually very small. On the other hand, the amounts of surfactant required for the formulation of a stable microemulsion of reverse phase are extraordinarily high and out of the technically relevant region. In addition, the reaction is usually started with a rather dilute solution of precursor salts, which does not make the outcome of inorganic particles very high.

In this paper, we present a novel technique which preserves some of the advantages of the inverse microemulsion route but requires minimized amounts of surfactant and allows high mass fluxes. As for the microemulsions, the final particles are accumulated in organic solvents, which diminishes corrosion and allows convenient further processing of the particles. The technique involves the transfer of the recently developed technique of inverse miniemulsions[6] to liquids with still higher cohesion energy, namely, molten salts or highly concentrated salt-containing ionic liquids. These miniemulsions can subsequently be further reacted to nanoparticles and nanostructures which can be highly melting and insoluble.

In the reported inverse miniemulsions, a liquid hydrophilic monomer was emulsified in a hydrophobic phase such as cyclohexane or other hydrocarbons by using high shear. The inverse miniemulsion obtains its stability by using a combination of an effective surfactant and an osmotic pressure agent, which is practically insoluble in the continuous phase and prevents the minidroplets from Ostwald ripening (in the case of inverse miniemulsions, this can be a salt). During the following conversions (e.g., polymerization, polyaddition), it was shown that each droplet can be considered as an independent nanoreactor, and ideally, the droplets convert in a one to one process under preservation of particle number and the amount of material in each droplet.

In this paper, it will be shown that concentrated salt solution or salt melts can indeed be miniemulsified,

* To whom correspondence should be addressed.

(1) Matijevic, E. *Chem. Mater.* **1993**, *5*, 412−426.
(2) Sharma, P. K.; Jilavi, M. H.; Burgard, D.; Nass, R.; Schmidt, H. *J. Am. Ceram. Soc.* **1998**, *81*, 2732−2734.
(3) Pileni, M. P. *Cryst. Res. Technol.* **1998**, *33*, 1155−1186.
(4) Hopwood, J. D.; Mann, S. *Chem. Mater.* **1997**, *9*, 1819−1828.
(5) Pileni, M. P. *Adv. Colloid Interface Sci.* **1993**, *46*, 139−163.
(6) Landfester, K.; Willert, M.; Antonietti, M. *Macromolecules* **2000**, *33*, 2370−2376.

10.1021/cm011121g CCC: $20.00 
Published on Web 10/09/2001

using appropriate block copolymers as surfactants. To underline the generality of the approach, we will perform a number of typical reactions with these nanodroplets leading to technologically relevant nanoparticles, namely, the precipitations toward oxides by addition of a base to the continuous phase ($ZrO_2$ and $Fe_3O_4$ needed as pigments, ceramic precursors, and magnetic materials) and by $CO_2$ adsorption from the gas phase leading to a very low-cost and side product-free synthesis of nanosized carbonates (here $CaCO_3$). Also, the miniemulsification of molten metals with high mass fractions in an organic phase will be introduced.

## Experimental Section

**Materials.** Iron(III) chloride hexahydrate, ethylbenzene, zirconyl chloride octahydrate, hexachloroplatinic acid hydrate, and calcium hydroxide were from Fluka. Pyridine, methoxyethylamine, samarium(III) nitrate hexahydrate, and hydrazine hydrate were purchased from Aldrich. Hydrochloric acid (0.1 M) was delivered by Riedel de Haen, and iron(II) chloride tetrahydrate was delivered by Merck. Gallium was received from Aldrich; Wood's metal and Rose's metal were received from Goodfellow. Cyclohexane was received from the BASF, and Isopar M was received from Exxon; both chemicals are of technical grade. The block copolymer emulsifier TEGO EBE45, consisting of a polystyrene block ($M_w$ = 3700) and a poly(ethylene oxide) block ($M_w$ = 3600), was kindly provided by Goldschmidt AG Essen. All chemicals were used as received without further purification.

**Analytical Methods.** The particle sizes were measured by dynamic light scattering using a Nicomp particle sizer (model 370, PSS Santa Barbara, USA) at a fixed scattering angle of 90°.

Electron microscopy was performed with a Zeiss 912 Omega electron microscope operating at 100 kV. The diluted colloidal solutions were applied to a 400+ mesh carbon-coated copper grid and left to dry; no further contrasting was applied.

The wide angle diffractograms were measured with a wide angle goniometer (Enraf-Nonius PS-120, Cu Kα) with a linear local sensitive detector. The samples were measured in reflection−transmission.

**Preparation of Nanosized Particles.** A 1 g portion of salt or an equal amount of high salt-containing polar solution was molten, by heating above the melting temperature, and added to 10 g of the continuous phase (e.g., cyclohexane or Isopar M) with varying amounts of TEGO EBE45 as an inverse stabilizer, with typically 0.1 g or 10 wt % of the phase to be dispersed. A stable miniemulsion was achieved by predispersion of the polar phase with a magnetic stirrer for 30 min and subsequent ultrasonication with a Branson W-450 with an amplitude of 90% for 2 min.

For base precipitation, 0.66 g of pyridine or 2-methoxyethylamine in 1 g of the continuous phase was added to the miniemulsion at room temperature under stirring. For carbonization, we made use of the rather high solubility of $CO_2$ in low polarity solvents by bubbling $CO_2$ through the miniemulsion.

## Results and Discussion

The extension of miniemulsions from water as a disperse polar phase to salt melts or concentrated salt solutions is not trivial, since those liquids show much higher cohesion energy, surface tension, and mutual attractions. This is why the steric stabilizer has to be well chosen; i.e., the polar part has to be miscible with the salt melts, whereas the unpolar part has to be sufficiently long and tightly packed to provide sufficient steric stabilization. For that, it turned out that amphiphilic block copolymers[7] with a poly(ethylene oxide) block are best suited. Here, we use an optimized precommercial block copolymer from the Goldschmidt AG (TEGO EBE45).

Another restriction of a liquid−liquid technology is that the melting point of the salt has to be at least lower than the boiling point of the continuous phase (boiling point range for Isopar M: 198−257 °C). This can be bypassed by using highly concentrated salt solutions or by adding impurities in the salts. If a system does not melt or dissolve under reasonable conditions, precursors have to be applied, which are later transferred in a particle-by-particle fashion to the final product. Here, salts or metals with relatively low melting points have been chosen: $Fe(III)Cl_3 \cdot H_2O$ (37 °C), $ZrOCl_2 \cdot 8H_2O$ (−6 $H_2O$, 150 °C), and $CaCl_2 \cdot 6H_2O$ (29.92 °C; −4 $H_2O$, 30 °C) and gallium (30 °C).

The liquid mixture is then subjected to very high shear, either by ultrasonication or by application of a microfluidizer in order to obtain small droplets.[8,9] To call an emulsion a "miniemulsion" rather than a macroemulsion, a number of characteristics have to be found.

Throughout the miniemulsification process, the droplet size runs into an equilibrium state. This "steady-state miniemulsion" is characterized by a dynamic rate equilibrium between fusion and fission of the droplets. Online turbidity and surface tension measurements allow the determination of the equilibrium state.

The nanodroplets have to be stabilized against Ostwald ripening by an osmotic agent which is practically insoluble in the continuous phase.

The surface coverage of the droplets with surfactant is incomplete and at the minimal value needed for particle stabilization under the applied conditions. With increasing amount of the surfactant, the particle size decreases.

**Preparation of Nanosized Iron Oxide $Fe_2O_3$.** Iron(III) chloride hexahydrate was melted above its melting temperature of 37 °C and added to the continuous phase using 5 wt % of TEGO EBE45 (with respect to salt) as stabilizer. A stable miniemulsion was achieved after ultrasonication. The process of miniemulsification was followed by turbidity measurements, and steady state was reached after about 200 s for this larger scale experiment. Decreasing the temperature leads to nanoscopic salt crystals being dispersed in a continuous oil phase. The average size of these particles is about 370 nm, as determined by dynamic light scattering. Due to the high density of the particles ($\rho$ ($FeCl_3$) = 1.82 g $cm^{-3}$), sedimentation occurs for days, but is reversible.

Addition of pyridine or methoxyethylamine to the cyclohexane−salt miniemulsion under stirring provides reaction to the iron(III) oxide with a particle size of about 330 and 370 nm, respectively. Here, the crystal water steps into the reaction, while pyridine from the continuous phase neutralizes the eliminated HCl. Obviously, the high interface area of the miniemulsion is high enough to allow this reaction.

Formation of $Fe_2O_3$ is accompanied with an increase in particle density ($\rho$ ($Fe_2O_3$) = 5.24 g $cm^{-3}$). The light scattering values and TEM pictures show that the

(7) Förster, S.; Antonietti, M. *Adv. Mater.* (*Weinheim, Ger.*) **1998**, *10*, 195.
(8) Bondy, C.; Söllner, K. *Trans. Faraday Soc.* **1935**, *31*, 835−842.
(9) Li, M. K.; Fogler, H. S. *J. Fluid Mech.* **1978**, *88*, 513−528.

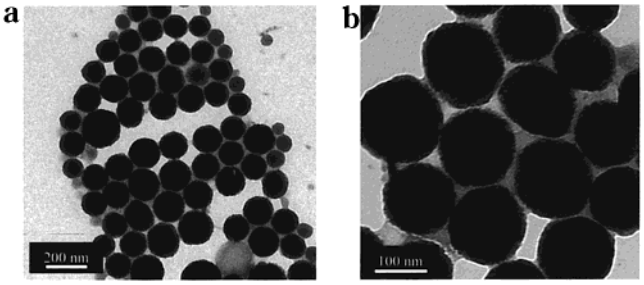


**Figure 1.** (a) Transmission electron micrograph of $Fe_2O_3$ in Isopar M obtained by miniemulsifying $FeCl_3$ with subsequent reaction. (b) Same picture as in (a) but with a higher magnification.

droplets do not shrink as a whole, but show aggregate structures with interstitial cavities between primary particles (Figure 1). The crystallinity of the particles was measured by wide angle X-ray scattering (WAXS). The crystallite sizes can be estimated from the line width of the WAXS peaks using the Scherrer equation; crystallite sizes of about 5 nm were detected.

For adjusting the particle size, the amount of surfactant and the oil composition as well as the chemical nature of the base were varied in a systematic fashion. These data are summarized in Table 1.

The efficiency of stabilization is related to solvent quality for the stabilizing block, while dielectric constant and refractive index difference determine the strength of colloidal interactions. With the use of cyclohexane as the continuous phase, stable miniemulsions of the primary salt emulsions (dispersions) were obtained, which were yellow orange and showed good stability with particle sizes ranging from 240 to 370 nm depending on surfactant concentration. The size of the primary salt dispersions generally decreases with increasing emulsifier content. By the addition of a base, particles with a size of about 250−380 nm were formed. The dispersion was of a brownish color.

Ethylbenzene, as the continuous phase, did result in dispersions with low stability. The emulsions were red brown with a particle size of about 300 nm. The particles formed by the addition of methoxyethylamine are unstable and settled quickly. With pyridine as the oxidizing base, smaller particles with a high polydispersity resulted, but the dispersions were not stable for long time.

Miniemulsions are also possible within the technically relevant petroleum ether Isopar M, where the particles are quite small and the dispersions become stable at very low amounts of surfactant (only 5 wt % with respect to salt). Also, the preparation of stable dispersions with a higher solid content of 23 wt % (Fe 60−Fe 62) is possible. In this case, the particle sizes are even smaller than in the dispersions with a solid content of 9 wt % (Fe 57−Fe 59 and Fe 63−Fe 65), which is probably due to the partitioning of TEGO EBE in the continuous phase. It has to be noted that as shown by interfacial tension measurements, the critical micelle concentration (cmc) of TEGO EBE in Isopar M is not reached; therefore, it is molecularly dissolved in the continuous phase without forming micelles. For higher solid contents, more surfactant can be adsorbed by the particles, and so, smaller particles can be obtained.

The size of the primary salt dispersions generally decreases with increasing emulsifier content. The size of the $Fe_2O_3$ particles after reaction is usually related to the primary droplet size, but in some cases, even disintegration toward smaller entities takes place. We attribute this behavior to the described shrinkage throughout the reaction and the fact that the less polar $Fe_2O_3$ is more easily dispersed in unpolar solvents than the precursor salt. This effect is more pronounced for methoxyethylamine as base which might contribute to surface stabilization.

**Table 1. Characteristics of the Nanoparticles at Different Emulsifier Concentrations before ($FeCl_3$) and after Reaction ($Fe_2O_3$)**

| | | | particle size (nm) | |
|---|---|---|---|---|
| expt | emulsifier (mg) TEGO EBE45 | base | $FeCl_3 \cdot 6H_2O$ particle | $Fe_2O_3$ particle |
| | *cyclohexane as continuous phase*, 1.5 g of $FeCl_3$, 15 g of cyclohexane | | | |
| Fe 51 | 75 (5%) | pyridine | 367 | 330 |
| | | MEA | | 377 |
| Fe 52 | 150 (10%) | pyridine | 319 | 278 |
| | | MEA | | 206 |
| Fe 53 | 300 (20%) | pyridine | 242 | 237 |
| | | MEA | | 249 |
| | *ethylbenzene as continuous phase*, 1.5 g of $FeCl_3$, 15 g of cyclohexane | | | |
| Fe 54 | 75 (5%) | pyridine | 318 | 367 |
| | | MEA | | |
| Fe 55 | 150 (10%) | pyridine | 284 | 407 |
| | | MEA | | |
| Fe 56 | 300 (20%) | pyridine | 328 | 299 |
| | | MEA | | |
| | *Isopar M as continuous phase*, 1.5 g of $FeCl_3$, 15 g of Isopar M | | | |
| Fe 57 | 75 | pyridine | 339 | 393 |
| | | MEA | | 389 |
| Fe 58 | 150 | pyridine | 223 | 265 |
| | | MEA | | 218 |
| Fe 59 | 300 | pyridine | 200 | 217 |
| | | MEA | | 191 |
| Fe 63 | 450 | pyridine | 164 | 184 |
| | | MEA | | 178 |
| Fe 64 | 600 | pyridine | 163 | 188 |
| | | MEA | | 159 |
| Fe 65 | 750 | pyridine | 156 | 182 |
| | | MEA | | 154 |
| | *Isopar M as continuous phase* (*high-concentration preparation*), 3 g of $FeCl_3$, 10 g of Isopar M | | | |
| Fe 60 | 150 | pyridine | 216 | 236 |
| | | MEA | | 206 |
| Fe 61 | 300 | pyridine | 181 | 205 |
| | | MEA | | 178 |
| Fe 62 | 500 | pyridine | 166 | 204 |
| | | MEA | | 162 |

**Preparation of Nanosized Magnetite $Fe_3O_4$ as a Ferrofluid.** The confinement of two species in stoichiometric amounts within the nanodroplets also allows the syntheses of mixed species, here, delineated for magnetite, $Fe_3O_4$. Because of the oxidizing ability of the ultrasonicating device, it is difficult to have, after the miniemulsification, the exact ratio of 2:1 needed for the preparation of magnetite by mixing the stoichiometric amounts of $Fe^{3+}$ and $Fe^{2+}$. Therefore, a highly concentrated solution of 1 g of Fe(II)−$SO_4$ and 0.8 g of 0.1 M hydrochloric acid was dispersed in 15 g of degassed Isopar M and 150 mg of TEGO EBE45. $N_2$ was bubbled through the mixture continuously to avoid the complete oxidation of $Fe^{2+}$ to $Fe^{3+}$. Only a part of $Fe^{2+}$ will be oxidized to $Fe^{3+}$ during ultrasonication, which allows magnetic particles to be obtained. After the mixture was

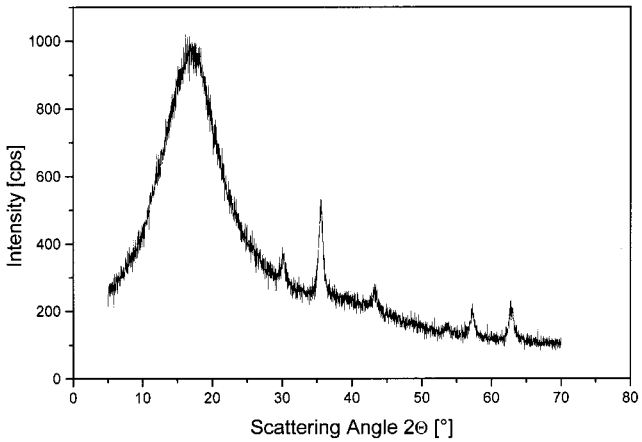


**Figure 2.** WAXS spectra of a dispersion of $Fe_3O_4$ in Isopar M. Note the detection of the Isopar M.

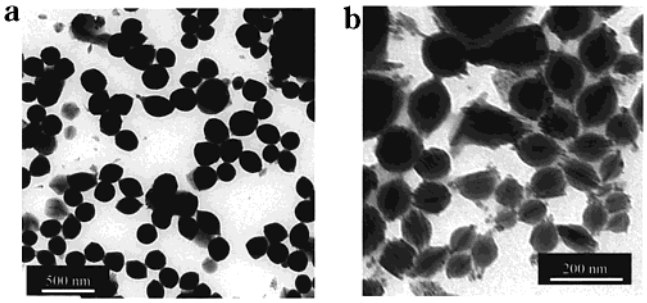


**Figure 3.** (a) TEM pictures of magnetite particles obtained by miniemulsion process. (b) Same sample as in (a) but at a higher magnification.

ultrasonicated, the miniemulsion was reacted by the quick addition of methoxyethylamine under stirring at 55 °C.

The final dispersion is black and shows magnetic properties. The saturation magnetization of the sample was 1 mT. The particle size is 200 nm. X-ray scattering on the dispersion revealed a crystalline structure with peaks (Figure 2) which correspond well with $Fe_3O_4$ spectra from the literature. The crystallite sizes can be estimated from the line width of the WAXS peaks using the Scherrer equation; crystallite sizes of about 12 nm were detected. As seen in the TEM pictures (Figure 3), the superstructure is anisotropic (lemon shaped), and the constituting nanocrystals can be identified inside the particles and are needle shaped, arranged as bundles along the main axis of the "lemons".

**Preparation of Nanosized Calcium Carbonate.** Calcium carbonate was made starting from calcium hydroxide or calcium chloride dihydrate. In the case of calcium hydroxide, a mixture of $Ca(OH)_2$ and $H_2O$ in the ratio of 1:2 enables a liquid starting situation. With 10 wt % of the emulsifier TEGO EBE45, the mixture was miniemulsified in cyclcohexane or Isopar M as a 25% dispersion.

In the case of calcium chloride dihydrate, only a very small amount of water was required to be able to miniemulsify the salt at 65 °C in cyclohexane or Isopar M. The size of the droplets that hardened at room temperature is 230 nm.

For the reaction of the calcium hydroxide or the calcium chloride to form calcium carbonate, carbon dioxide was bubbled through the prepared miniemulsion

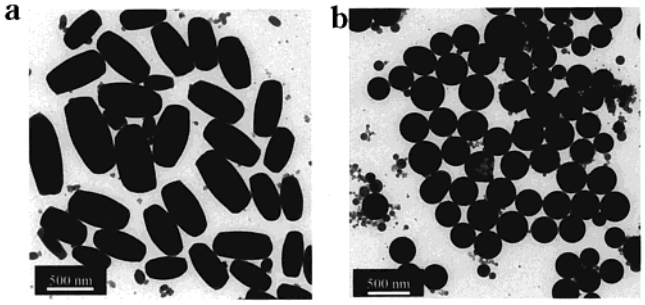


**Figure 4.** (a) TEM photographs of $ZrOCl_2$ particles obtained in a miniemulsion process. (b) TEM photographs of $ZrO_2$ particles obtained after reaction from the particles in (a).

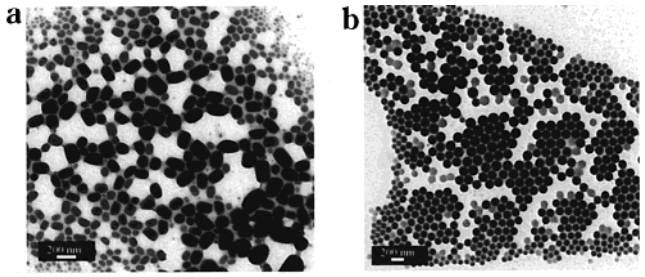


**Figure 5.** TEM photographs of $ZrOCl_2$: (a) crystallization by decreasing the temperature at a $ZrOCl_2$ octahydrate/water ratio of 1:0.8; (b) stripping out the water of this miniemulsion at 80 °C.

under stirring at room temperature to get calcium carbonate with a particle size of 280 nm (from $Ca(OH)_2$) and 289 nm (from $CaCl_2$). In the case of $CaCl_2$, pyridine was added to neutralize the forming acid. The increase in size is due to the serious mass uptake of the particles from the continuous phase.

**Preparation of Nanosized Zirconium Dioxide.** Pure zirconyl chloride octahydrate melts and degrades at 150 °C, but the melting temperature of the salt can easily be reduced by adding water to the salt. A 3:1 $ZrOCl_2$/water mixture melts at about 70 °C. The molten salt was added to Isopar M at 75 °C. A stable miniemulsion was obtained using 10 wt % of TEGO EBE45, which transforms throughout cooling in a dispersion of single $ZrOCl_2$ nanocrystals as shown by WAXS measurements. TEM pictures show (see Figure 4a) that the particles are of uniform polyhedral crystalline shape.

Methoxyethylamine was added under stirring to the miniemulsions with molten droplets, which are spherical, and polycrystalline zirconium dioxide spheres with a particle size of 260 nm are obtained (see Figure 4b).

Again, the presence of hollow particles indicates that the spherical superstructure is composed of smaller nanoparticles and contains cavities due to the shrinking throughout the reaction.

A higher water content for the formulation of the $ZrOCl_2$ miniemulsion (weight ratio of 1:1) results, after water is stripped out ($ZrOCl_2$/water weight ratio of 1:0.8) and after subsequent cooling, in particles with different shapes (Figure 5a). When the water from this miniemulsion is stripped out constantly at a temperature of 80 °C, spherical particles are obtained (Figure 5b), which are presumably superstructures of much smaller nanocrystals. These dispersions look rather perfect for further ceramic processing.

**Preparation of Metallic Nanoparticles by the Miniemulsion Process.** For the preparation of nano-

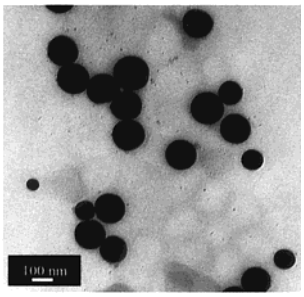


**Figure 6.** Particles from Wood's metal in Isopar M, sample Wood 6.

sized metal dispersions, the same procedure of high shear forces was used to prepare miniemulsions. Molten metals have very strong cohesion forces, which make them very difficult to disperse in an organic phase by conventional techniques.

Low-melting metals and alloys can be used to prepare the described type of miniemulsions. A 1 g portion of gallium (mp = 30 °C) was molten at 45 °C, and 10 g of Isopar M and 100 mg of TEGO EBE45 were added. After pre-emulsification for 30 min at high speed, subsequent ultrasonication lead to a stable miniemulsion. The miniemulsion was cooled to room temperature, and solid gallium particles with a size of 150 nm were obtained. The same experiment in cyclohexane resulted in a stable dispersion with larger particles of 240 nm. The reasons for the lower dispersion efficiency in cyclohexane were discussed above.

The same procedure can be applied to disperse low-melting alloys like Wood's metal (composition: Bi, 50; Pb, 25; Cd, 12.5; Sn, 12.5) (mp = 70 °C) or Rose's metal (composition: Bi, 50; Pb, 28; Sn, 22) (mp = 110 °C). Because of the very high density difference of the metal ($\rho$ (Wood's metal) = 9.67 g cm$^{-3}$) and the continuous phase ($\rho$ (Isopar M) = 0.87 g cm$^{-3}$), the weight content of the metal was increased to 50 wt % to obtain relevant volume fractions (for TEM see Figure 6). The resulting dispersions are still stable, and their average density was determined to be 1.325 g cm$^{-3}$, which goes well with the number calculated from the stoichiometry. All other data are summarized in Table 2.

The application of these metal dispersions on paper as conducting ink results after evaporation of the solvent in films with metallic gloss and rather high conductivities, which cannot be quantified due to the ill-defined metal−paper geometry. For such experiments, the lowest surfactant concentration of 10 wt % with respect to metal seems to be the best suited, since the lower layer thickness of the potentially insulating polymer surfactant leads to better particle contacts and higher conductivities.

**Table 2. Various Metal Dispersions Prepared in Isopar M with Different Amounts of TEGO EBE45 as Surfactant**

| expt | metal (g) | | TEGO EBE45 (g) | Isopar M (g) | particle size (nm) |
|---|---|---|---|---|---|
| Ga1 | gallium | 1.48 | 0.10 | 10.0 | 146 |
| Ga2 | gallium | 1.05 | 0.10 | 11.0 (CH) | 235 |
| Wood 1 | Wood's metal | 2.15 | 0.20 | 20.0 | 350 |
| Wood 3 | Wood's metal | 14.43 | 0.15 | 15.3 | 286 |
| Wood 4 | Wood's metal | 15.60 | 0.60 | 15.0 | 206 |
| Wood 5 | Wood's metal | 13.43 | 1.00 | 14.7 | 216 |
| Wood 6 | Wood's metal | 15.28 | 1.20 | 15.5 | 230 |
| Rose 3 | Rose's metal | 16.79 | 0.17 | 16.9 | 263 |

## Conclusion

It was shown that the miniemulsification of low-melting salts and metals enables the direct synthesis of nanoparticles of high homogeneity with diameters between 150 and 400 nm. Application of appropriate steric stabilizers makes those dispersions colloidally stable in nonpolar organic solvents. In the dispersed state, heterophase reactions such as precipitations, oxidations, or carbonizations can be performed, which essentially occur under preservations of the colloidal entities as single nanoreactors.

Due to the simplicity of liquid−liquid reactions, the quality of the particle size distributions, and the smoothness of the particle surfaces, the presented technique is a considerable alternative to other techniques of colloid generation, such as milling or controlled precipitation reactions.

As model cases, we choose the syntheses of a pigment ($Fe_2O_3$), magnetic nanoparticles ($Fe_3O_4$), an abrasive ($CaCO_3$), a ceramic precursor ($ZrO_2$), and low-melting metals used in electric fuses.

Such dispersions have a whole range of applications in materials, for instance, in electronic inks. The use of these dispersions in printing devices offers the advantage that the printed structures are functional, e.g., they are magnetic or electronically conducting.

This is why we believe that miniemulsion technologies will also gain importance in the field of nanostructured solid materials.

**Acknowledgment.** The authors thank Rona Pitschke for the TEM measurements and the Max Planck Society for financial support.

CM011121G